

# The Geometric Influence of the Tubular-Hat Tube on Its Energy Absorption Capacity in Axial Load

Hung Anh Ly, Thanh Tien Pham

Department of Aerospace Engineering, Ho Chi Minh City University of Technology, Ho Chi Minh City, Vietnam

## Email address:

lyhunganh@hcmut.edu.vn (H. A. Ly), phamthanhtien5789@gmail.com (T. T. Pham)

## To cite this article:

Hung Anh Ly, Thanh Tien Pham. The Geometric Influence of the Tubular-Hat Tube on Its Energy Absorption Capacity in Axial Load. *International Journal of Transportation Engineering and Technology*. Special Issue: Experiments Researches in Aeronautical Engineering. Vol. 2, No. 5-1, 2016, pp. 12-17. doi: 10.11648/j.ijtet.s.2016020501.13

**Received:** August 12, 2016; **Accepted:** October 9, 2016; **Published:** November 22, 2016

**Abstract:** Crashworthiness is an important criterion in vehicle design. In fact, a crashworthy design will reduce the terrible accidents that happen everyday. Normally, tube structures are used for this task by dissipating the impact energy on the folding waves formed during the crushing progress. This study continues the previous studies, focuses on analyzing the behavior of tubular-hat subjected to axial collision. Because of the limitations on the experimental conditions, and by the finite element method, this study only concentrates on the tube section. There are two main objectives in this thesis. Firstly, we consider the difference between the behaviors of the top-hat tube and of the double-hat tube with the same axial load. Then, the geometric influence of flange on the deformation of the tubular-hat is investigated.

**Keywords:** Crashworthiness, Top-Hat, Double-Hat, Impact, Optimization

## 1. Introduction

### Background

Crashworthiness is an important criterion for the vehicle choice. It is the ability to protect the passengers in the case of collision. A crashworthy design will ensure the safety for passengers. For example, in spite of a car impacts at a high speed, the driver is still safe thanks to the seatbelts. Besides, the car structure absorbs and dissipates the impact energy.

In the structure design, crashworthiness relates to the energy absorption of the structure. The impact energy is absorbed on the folding wave of the thin-walled structure. To make the design process easier, these structure behaviors have been studied for many years.



Figure 1. NASA's helicopter drop test [1].

This study continues some previous works and focuses on analyzing the behavior of tubular-hat subjected to axial collision. Objectives in this paper: the influence of the flange geometry on the deformation of the tubular-hat is investigated.

### Method of approach

Due to the limitations in terms of experimental conditions, this study focuses on analyzing the behaviors of the top-hat and double-hat sections by the theoretical analysis and the simulation with the Finite Element Method (FEM). Thus, the explicit finite element software LS-DYNA is used

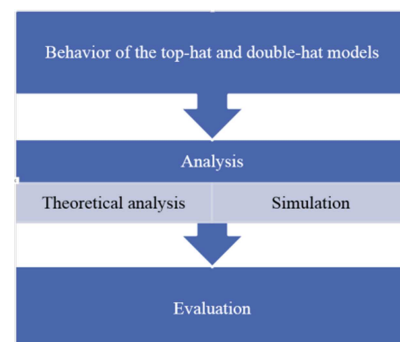


Figure 2. Method of approach.

## 2. Theoretical Background

The theoretical analysis of M. White, N. Jones and W. Abramowicz [2] [3]

Analytical solution for the quasi-static axial crushing force of top-hat and double-hat sections

Top-hat section

Cross-section of a top-hat tube

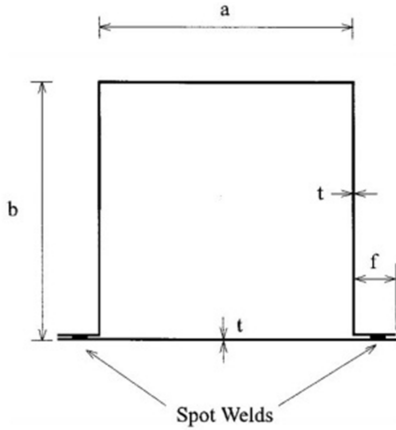


Figure 3. Cross-section of a top-hat column [2].

$$L = 2a + 2b + 4f \tag{1}$$

Simplified solution for strain hardening materials

$$\frac{\bar{P}_m}{M_u} = 35.55 \left( \frac{L}{t} \right)^{0.29} \tag{2}$$

$$\frac{H}{t} = 0.478 \left( \frac{L}{t} \right)^{0.64} \tag{3}$$

$$\frac{r}{t} = 0.563 \left( \frac{L}{t} \right)^{0.32} \tag{4}$$

Double-hat section

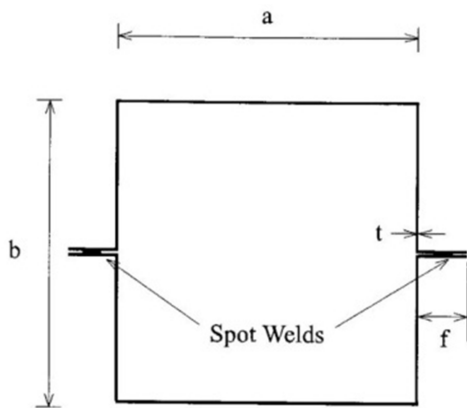


Figure 4. Cross-section of double-hat column [3].

Simplified solution for strain hardening materials

$$\frac{\bar{P}_m}{M_u} = 58.15 \left( \frac{L}{t} \right)^{0.29} \tag{5}$$

$$\frac{H}{t} = 0.532 \left( \frac{L}{t} \right)^{0.64} \tag{6}$$

$$\frac{r}{t} = 0.45 \left( \frac{L}{t} \right)^{0.32} \tag{7}$$

Analytical solution for the dynamic axial crushing of top-hat and double-hat thin-walled sections

Top-hat section

$$\left( \frac{\bar{P}_m}{P_m} \right)^d = 1 + \left( 0.87 \frac{V}{L^{0.96} t^{0.04} D} \right)^{\frac{1}{P}} \tag{8}$$

Double-hat section

$$\left( \frac{\bar{P}_m}{P_m} \right)^d = 1 + \left( 0.973 \frac{V}{L^{0.96} t^{0.04} D} \right)^{\frac{1}{P}} \tag{9}$$

## 3. Influence of Flange Location to Tubular-Hat

Geometric

In this research, the behavior of tubular-hat structure is studied. The configuration of tubular-hat section is demonstrated in Figure 5.  $a=50\text{mm}$ ,  $t=1.1\text{mm}$ . The flange width  $f$  is chosen as 15 mm. The other dimensions,  $h$  and  $b$ , are listed in Table 1.

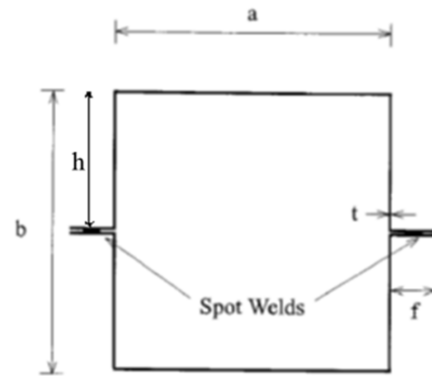


Figure 5. Dimensions of tubular-hat.

Table 1. Dimensions of tubular-hat.

| No. | $h/b$ | $h(\text{mm})$ | $b(\text{mm})$ |
|-----|-------|----------------|----------------|
| 1   | 0.0   | 0              | 50             |
| 2   | 0.1   | 5              | 50             |
| 3   | 0.2   | 10             | 50             |
| 4   | 0.3   | 15             | 50             |
| 5   | 0.4   | 20             | 50             |
| 6   | 0.5   | 25             | 50             |

*Mesh size*

The Belytschko-Tsay 4-node shell elements with 5 integration points are used to model column wall with the finer mesh size (2×2 mm).

*Boundary and condition contact*

In this study, we just examine the case of axial loading. Therefore, the indenter is only permitted to displace in z-axis. For the tube, the nodes in the lowest cross section are clamped. The indenter is set initial velocity V=8m/s.

The spot-weld is a rigid 4-solid that connects the nodal pairs between two sheets as shown in Figure 6. Spot-weld is assumed that can not be broken, and the spot-weld pitch is equaled to the mesh-size (2 mm). The distance between the two surface is the thickness of plate.

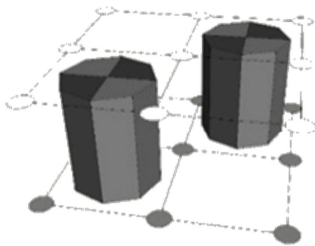


Figure 6. Surface node 4-solid elements model of two spot-welds.

The models in this study use two contact algorithms. The contact between the indenter and the tube is AUTOMATIC\_NODES\_TO\_SURFACE. Its static coefficient and dynamic coefficient of friction are 0.4 and 0.3. The contact AUTOMATIC\_SINGLE\_SURFACE is used for the tube wall to avoid interpenetration of tube wall other.

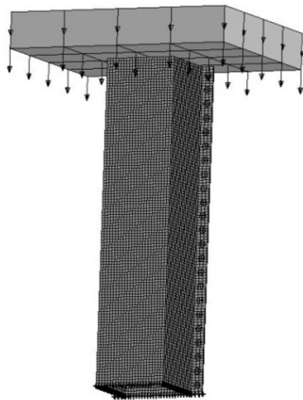


Figure 7. Boundary condition of top-hat.

*Characteristics of materials*

In this study, the wall tube material is mild steel RSt37 which was used by S. P. Santosa *et al.* [4] in the studies about foam-filled thin-walled column with mechanical properties: Young’s modulus  $E = 200GPa$ , initial yield stress  $\sigma_y = 251MPa$ , ultimate stress  $\sigma_u = 339MPa$ , Poisson’s ratio  $\nu = 0.3$ , density  $\rho = 7830kg/m^3$ , and the power law exponent  $n = 0.12$ . The empirical Cowper-Symonds uniaxial constitutive equation constants  $D = 6844s^{-1}$  and  $p = 3.91$ . The material model used to simulate mild steel is Type 24

MAT\_PIECEWISE\_LINEAR\_PLASTICITY – an elasto-plastic material with an arbitrary stress versus strain curve and arbitrary strain rate dependency. The true stress – effective plastic strain curve of RSt37 steel was calculated by H. A. Ly. [5] from the engineering stress-strain curve of Santosa and was given in Table 2. The material model used for indenter is  $\rho = 1.4e-4kg/mm^3$ , mass is 114,2kg with Young’s modulus  $E = 200GPa$  and Poisson’s ratio  $\nu = 0.3$ .

The material model used for spot-weld is mild steel Rst37

Table 2. True stress- Effective plastic strain data of mild steel RSt37 [5].

| Mild steel RSt37             |                           |
|------------------------------|---------------------------|
| Effective plastic strain (%) | True plastic stress (MPa) |
| 0.0                          | 251                       |
| 2.0                          | 270                       |
| 3.9                          | 309                       |
| 5.8                          | 339                       |
| 7.7                          | 358                       |
| 9.6                          | 375                       |
| 11.4                         | 386                       |
| 13.2                         | 398                       |

*Result of simulation using LS-DYNA*

Table 3. Mean crushing force and displacement of six models tubular-hat.

| No. | $h/b$ | $(\bar{P}_m)^d$ (kN) | Displacement (mm) |
|-----|-------|----------------------|-------------------|
| 1   | 0.0   | 23.85                | -153.78           |
| 2   | 0.1   | 28.37                | -129.09           |
| 3   | 0.2   | 33.80                | -108.41           |
| 4   | 0.3   | 34.93                | -104.92           |
| 5   | 0.4   | 35.57                | -104.82           |
| 6   | 0.5   | 37.64                | -105.08           |

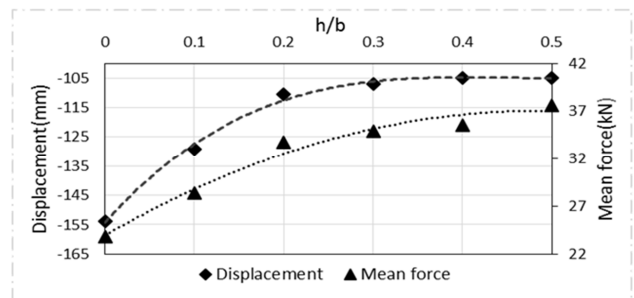


Figure 8. Relationship between mean crushing force, displacement and the ratio of h/b of tubular-hat specimen.

The ratio h/b increases, the instantaneous force, mean force increase and displacement decrease. The ratio of h/b=0.5 gives the highest values of instantaneous force and mean force.

### 4. Influence of Flange Length to Tubular-Hat Tube

*Geometric of models*

- Model (M1)- Perimeter 300mm

The values of a, b, t and f are given in Table 4. The length of models is 270mm. The perimeter of top hat tube is 300mm.

**Table 4.** Geometry of top-hat (models (M1)).

| No. | a (mm) | b (mm) | t (mm) | f (mm) |
|-----|--------|--------|--------|--------|
| 1   | 65     | 65     | 1.5    | 10     |
| 2   | 63     | 63     | 1.5    | 12     |
| 3   | 62     | 62     | 1.5    | 13     |
| 4   | 61     | 61     | 1.5    | 14     |
| 5   | 60     | 60     | 1.5    | 15     |
| 6   | 59     | 59     | 1.5    | 16     |
| 7   | 57     | 57     | 1.5    | 18     |
| 8   | 55     | 55     | 1.5    | 20     |
| 9   | 53     | 53     | 1.5    | 22     |

- Model (M2)- Perimeter 350mm

The values of a, b, t and f are given in Table 5. The length of models is 270mm. The perimeter of top hat is 350mm.

**Table 5.** Geometry of top-hat (model(M2)).

| No. | a (mm) | b (mm) | t (mm) | f (mm) |
|-----|--------|--------|--------|--------|
| 11  | 73.5   | 73.5   | 1.5    | 14     |
| 12  | 71.5   | 71.5   | 1.5    | 16     |
| 13  | 69.5   | 69.5   | 1.5    | 18     |
| 14  | 67.5   | 67.5   | 1.5    | 20     |
| 15  | 65.5   | 65.5   | 1.5    | 22     |
| 16  | 63.5   | 63.5   | 1.5    | 24     |

**Materials**

The material parameter used for the indenter in model (M1) is  $\rho=1.84e-4kg/mm^3$ , the mass is 151.13kg with the Young's modulus  $E=200GPa$  and the Poisson's ratio  $\nu=0.3$ .

The material parameter used for indenter in model (M2) is  $\rho=2.16e-4kg/mm^3$ , the mass is 176.24kg with the Young's modulus  $E=200GPa$  and the Poisson's ratio  $\nu=0.3$ .

**Numerical results**

- Model (M1)- Perimeter 300mm

The simulation results of the top-hat specimen with the geometric dimensions given in Table 4 include the displacement in Table 6 and Figure 9 and the crushing force in Table 7 and Figure 10. In Figure 10, the analytical mean crushing force (White & Jones) line is predicted by using Eqs.(2) and (8)

**Table 6.** Displacement of some models top-hat,  $L=300mm$ .

| No. | 4f/L  | f (mm) | Displacement (mm) |
|-----|-------|--------|-------------------|
| 1   | 13.33 | 10     | -120.27           |
| 2   | 16    | 12     | -119.26           |
| 3   | 17.33 | 13     | -119.76           |
| 4   | 18.67 | 14     | -112.97           |
| 5   | 20    | 15     | -116.17           |
| 6   | 21.33 | 16     | -120.76           |
| 7   | 24    | 18     | -123.48           |
| 8   | 26.67 | 20     | -127.61           |
| 9   | 29.33 | 22     | -129.78           |

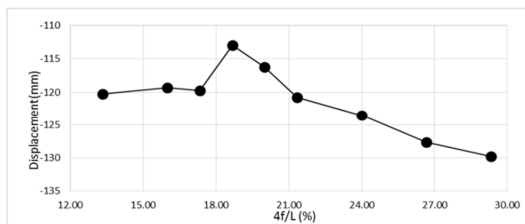


**Figure 9.** Influence of 4f/L ratio to displacement,  $L=300mm$ .

We found that the displacement is shortest if  $f = 14mm$ ,  $4f/L = 18.67\%$ . When  $f$  increases, the deformation increases

**Table 7.** Crushing force of some top-hat models,  $L=300mm$ .

| No. | 4f/L  | f (mm) | Crushing force (kN) |
|-----|-------|--------|---------------------|
| 1   | 13.33 | 10     | 41.06               |
| 2   | 16    | 12     | 41.39               |
| 3   | 17.33 | 13     | 41.20               |
| 4   | 18.67 | 14     | 43.78               |
| 5   | 20    | 15     | 42.53               |
| 6   | 21.33 | 16     | 40.86               |
| 7   | 24    | 18     | 39.93               |
| 8   | 26.67 | 20     | 38.64               |
| 9   | 29.33 | 22     | 37.98               |

The analytical mean crushing force is (White & Jones)  $P_m = 39.279kN$

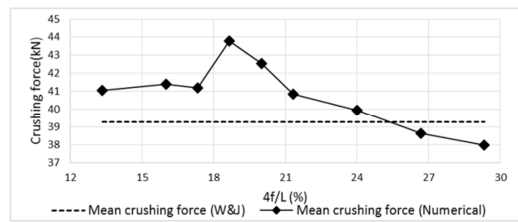


**Figure 10.** Influence of 4f/L to crushing force,  $L=300mm$ .

- Model (M2)- Perimeter 350mm

The simulation results of the top-hat specimen with the geometric dimensions given in Table 4 include the displacement in Table 8 and Figure 11 and the crushing force in Table 9 and Figure 12.

**Table 8.** Displacement of some top-hat models,  $L=350mm$ .

| No. | 4f/L  | f (mm) | Displacement (mm) |
|-----|-------|--------|-------------------|
| 11  | 16    | 14     | -134.48           |
| 12  | 18.29 | 16     | -131.63           |
| 13  | 20.57 | 18     | -134.12           |
| 14  | 22.86 | 20     | -112.97           |
| 15  | 25.14 | 22     | -116.17           |
| 16  | 27.43 | 24     | -120.76           |

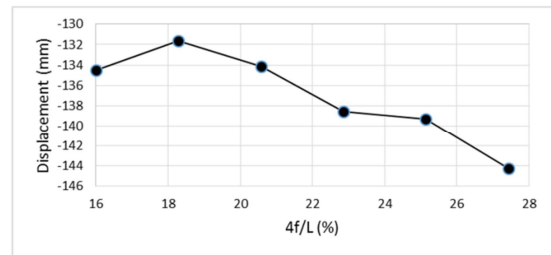


**Figure 11.** Influence of 4f/L ratio to displacement,  $L=350mm$ .

**Table 9.** Crushing force of some model top-hat,  $L=350mm$ .

| No. | 4f/L  | f (mm) | Crushing force (kN) |
|-----|-------|--------|---------------------|
| 11  | 16    | 14     | 42.98               |
| 12  | 18.29 | 16     | 43.97               |
| 13  | 20.57 | 18     | 43.09               |
| 14  | 22.86 | 20     | 41.69               |
| 15  | 25.14 | 22     | 41.53               |
| 16  | 27.43 | 24     | 39.95               |

The analytical mean crushing force (White & Jones)  $P_m = 40.773kN$

We found that the tube displacement is minimal when  $f = 16\text{mm}$ , or  $4f/L = 18.29\%$ . If  $f$  increases, the deformation increases.

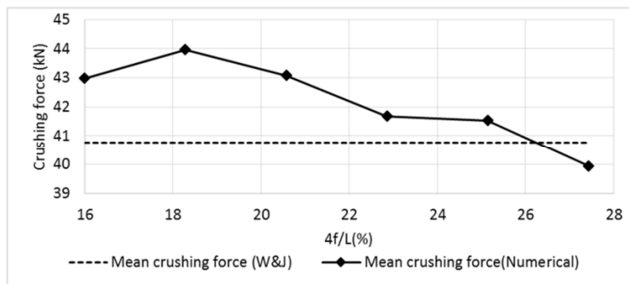


Figure 12. Influence of  $4f/L$  to crushing force,  $L=350\text{mm}$ .

## 5. Conclusion

When the ratio of  $h/b$  increases, the maximum of instantaneous force is increases. The ratio of  $h/b=0.5$  gives

## Nomenclature

|                 |  |                 |
|-----------------|--|-----------------|
| $a$             | Width of a top-hat or double-hat section                   | m               |
| $b$             | Depth of a top-hat or double-hat section                   | m               |
| $D, p$          | Cowper-Symonds coefficients                                | $s^{-1}, -$     |
| $E$             | Young's modulus  | Pa              |
| $f$             | Width of flange  | m               |
| $L$             | Perimeter of a top-hat or double-hat section               | m               |
| $M_u$           | $0.25\sigma_u t^2$   | N               |
| $\bar{P}_m$     | Mean static crushing force for a strain hardening material | N               |
| $(\bar{P}_m)^d$ | Mean dynamic crushing force                                | N               |
| $r$             | Rolling radius of toroidal surface                         | m               |
| $t$             | Thickness of section                                       | m               |
| $\rho$          | Density of material  | $\text{kg/m}^3$ |
| $\sigma_y$      | Yield stress   | Pa              |
| $\sigma_u$      | Ultimate stress  | Pa              |
| $\nu$           | Poisson's ratio  | -               |

## Acknowledgments

The authors acknowledge the support from the Ho Chi Minh city University of Technology for provision of research grants.

## References

- [1] B. Dickey and K. Barnstorff, *Chopper Drop Tests New Technology*, NASA, 12 August 2009. [Online]. Available: [http://www.nasa.gov/topics/aeronautics/features/helodroptest\\_prt.htm](http://www.nasa.gov/topics/aeronautics/features/helodroptest_prt.htm).
- [2] M. White, N. Jones and W. Abramowicz, A theoretical analysis for the quasi-static axial crushing of top-hat and double-hat thin-walled sections, *International Journal of Mechanical Sciences*, 1999, vol. 41: 209-233.
- [3] M. White and N. Jones, A theoretical analysis for the dynamic axial crushing of top-hat and double-hat thin-walled sections, *Proceedings of the Institution of Mechanical Engineers*, 1999, vol. 213: 307-325.
- [4] S. P. Santosa, T. Wierzbicki, A. G. Hanssen and M. Langseth, Experimental and numerical studies of foam-filled sections, *International Journal of Impact Engineering*, 1999, 24: 509-534.
- [5] A. H. Ly, *Behavior of thin-walled prismatic structures subjected to low velocity impact loading*, M. A. Thesis, Institut Teknologi Bandung, Indonesia, 2007.
- [6] K. Wilkinson, What is resistance spot welding? *Trade Equipment*, 13 April 2011. [Online]. Available: <http://www.trade-equip.co.uk/blog/?p=289>

the highest value of instantaneous force and mean force. By comparing a top-hat tube and a double-hat tube with the same boundary condition and perimeter. We found that the crushing force of double - hat tube is higher than top - hat section. When displacement is same, if  $4f/L \approx 18\%$ , the energy absorption capacity of top-hat tube is the highest.

## Achievement and Limitation

When the ratio of  $h/b$  increases, the maximum of instantaneous force is increases. The ratio of  $h/b=0.5$  gives the highest value of instantaneous force and mean force. If  $\frac{4f}{L} \approx 18\%$ , the energy absorption capacity of top-hat tube is the highest.

In this research, the mechanical properties of the spot-weld material is not considered because of the lack of experimental data. The results of the ratio  $\frac{4f}{L}$  are not tested experimentally

## Biography



**Hung Anh LY** is a Lecturer in the Department of Aerospace Engineering – Faculty of Transport Engineering at Ho Chi Minh City University of Technology (HCMUT). He received his BEng in Aerospace Engineering from HCMUT in 2005, his MEng in Aeronautics and Astronautics Engineering from Bandung Institute of Technology - Indonesia (ITB) in 2007 and his DEng in Mechanical and Control Engineering from Tokyo Institute of Technology – Japan (Tokyo Tech) in 2012. He stayed at ITB and Tokyo Tech for one month as a researcher in 2012 and 2013. He is a member of the New Car Assessment Program for Southeast Asia (ASEAN NCAP). His main research interests include strength of structure analysis, impact energy absorbing structures and materials.



**Thanh Tien PHAM** is currently a final-year student at the Department of Aerospace Engineering, Faculty of Transportation Engineering, Ho Chi Minh City University of Technology (HCMUT), Vietnam. He is going to receive the Bachelor's degree in Aerospace Engineering from HCMUT in April, 2016. His research interests include the areas of structural impact and finite element methods.